Molecular Crystals and Liquid Crystals Science and Technology. Section A. Molecular Crystals and Liquid Crystals
Publication details, including instructions for authors and subscription information:
http://www.tandfonline.com/loi/gmcl19

Transient Patterns in the Magnetic Reorientation of Low Molecular Mass Nematic Liquid Crystals

M. Grigutsch [a], N. Klöpper [a], H. Schmiedel [a] & R. Stannarius [a]
[a] Universität Leipzig, Fakultät für Physik und Geowissenschaften Linnéstr, 5, 0-04103, Leipzig, Germany
Version of record first published: 23 Sep 2006.

To cite this article: M. Grigutsch , N. Klöpper , H. Schmiedel & R. Stannarius (1995): Transient Patterns in the Magnetic Reorientation of Low Molecular Mass Nematic Liquid Crystals, Molecular Crystals and Liquid Crystals Science and Technology. Section A. Molecular Crystals and Liquid Crystals, 261:1, 283-292

To link to this article: http://dx.doi.org/10.1080/10587259508033475

Mol. Cryst. Liq. Cryst. 1995, Vol. 261, pp. 283–292
Reprints available directly from the publisher
Photocopying permitted by license only

TRANSIENT PATTERNS IN THE MAGNETIC REORIENTATION OF LOW MOLECULAR MASS NEMATIC LIQUID CRYSTALS

M. GRIGUTSCH, N. KLÖPPER, H. SCHMIEDEL, and R. STANNARIUS
Universität Leipzig, Fakultät für Physik und Geowissenschaften
Linnéstr. 5, D-04103 Leipzig, Germany

Abstract

We present the results of optical investigations of transient patterns appearing during the reorientation of nematic LC in magnetic fields. The transition from a planar modulated director field to a metastable non-planar structure of twist-bend walls is observed. From the wavelengths and characteristic rise times of the investigated patterns, the validity of the linearized mode selection theory is confirmed and viscoelastic parameters are determined.

INTRODUCTION

As a consequence of the symmetry of the nematic phase, the director reorientation in an external (electric or magnetic) field perpendicular to the initial director is connected with a spontaneous local symmetry breaking, as e.g. in the Fréedericksz transition. Far from equilibrium, that is at strong external fields, nematodynamics is highly non-linear and it is characterized by a strong coupling of gradients of director reorientation and mass flow field. At supercritical field strenghts, the spontaneous formation of transient patterns is observed. The wavelengths of the patterns increase with decreasing field strength and diverge in the vicinity of the critical field. The onset of the instability has been described by Guyon and co-workers [3] in terms of a deterministic linear stability analysis (LSA) which was found to be in qualitative agreement with experimental observations [4,5,6]. Modifications of the LSA have been proposed by Srajer et al. [2] and Sagúes and co-workers [7] in order to take into account non-linear effects and thermal fluctuations.

We have studied the formation and the long-term behaviour of transient patterns in the magnetic twist Fréedericksz transition of low molecular mass nematics. The evolution of the transient textures has been directly observed by optical microscopy in a magnetic field. We have obtained information on pattern growth rates, the characteristics of the director deformations involved and the macroscopically observed

wavelengths in dependence upon time. The measured periodicities and growth rates of the patterns in the limit of small director deformations, that is short after the onset of the instability, are compared with the predictions from the LSA.

EXPERIMENTAL

Sandwich cells with cell gaps between 25 and 250 μm have been filled with the nematic LC. By appropriate surface treatment (SiO_x-evaporation or polyimid coating and rubbing) a homogeneous planar director alignment is achieved. The sample cells are exposed to a stabilizing magnetic field (field direction along the easy axis $\vec{n}_0$) and then flipped by an angle of $\pi/2$ around an axis normal to the cell plane. The flip has to be fast as compared to the director reorientation time of the sample. Alternatively, the cells can be placed between the poles of the electromagnet at zero field and the magnetic field is switched on perpendicular to $\vec{n}_0$. In both experiments, the geometry of a twist Fréedericksz transition is realized. The transient textures evolving in the cell plane during the director reorientation are recorded by means of a video camera with a frame rate of 25/s. The camera is mounted on top of a microscope placed between the magnetic pole shoes above the sample cell. For details see refs. [8,9].
The substances investigated are a four component mixture of alkyloxy-phenylbenzoates (Mi5) [8] and another four component mixture of naphtyl derivatives E2 [10]. The latter shows a glass transition in the nematic phase and a variation of the viscosity coefficients and consequently of the relaxation times over several decades.

RESULTS

Optical textures typically observed in thin sample cells (cell gap $< 100\mu m$) are shown in Fig. 1 together with the contour plots of the 2D Fourier transforms of the images. The images were taken with crossed polarizers in 0°-position to the easy axis $\vec{n}_0$ and a $\lambda/4$-plate inserted at 45° to $\vec{n}_0$. Alternating bright and dark stripes indicate a periodic arrangement of domains with opposite sense of director reorientation. From the Fourier transform a uniform wavelength of the pattern is found with wavevector $\vec{q} \parallel \vec{n}_0$. With progressing time the image contrast increases and (at sufficiently strong external fields) the characteristics of the texture finally alter. The optical images of the domain borders emerge from their surroundings and generate a second peak in the Fourier spectrum at about half the wavelength of the previous image.

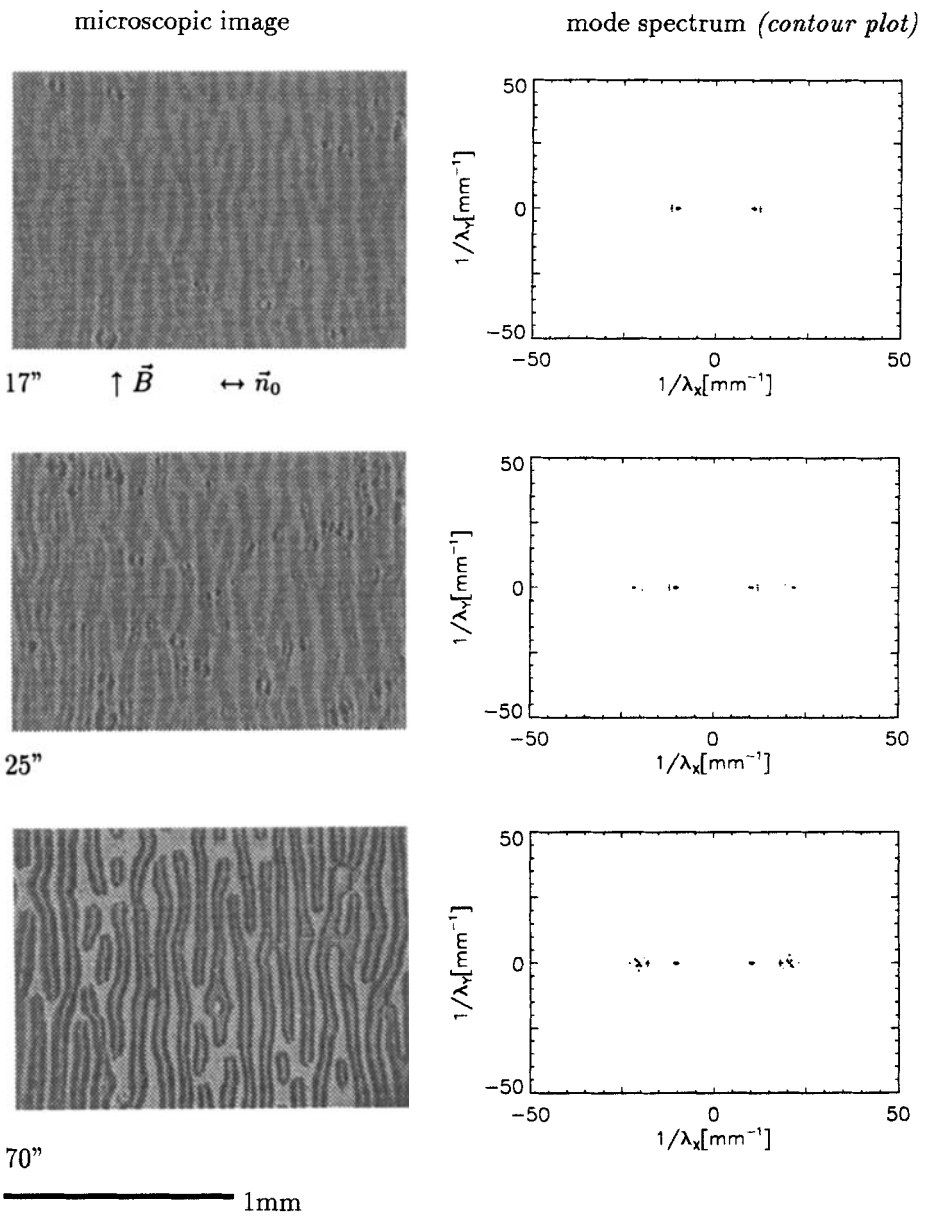

Figure 1: Transient patterns in the magnetic twist reorientation Sample: *E2* [10], $T = 91°C$, $d = 40.14\mu m$, $B = 500mT$, the coordinate x is along $\vec{n}_0$ and z is normal to the cell plane.

If now the analyzer is removed from the optical setup, the domain borders are still visible indicating that their images result from light focussing effects. Without polarizers there is, however, no optical contrast between domains of opposite director

twist. Consequently, the first peak in the Fourier spectrum is absent. In thick sample cells, only the second type of textures is observed. Due to wave guiding [8], there is no optical contrast between the twist domains even with the polarizers inserted.

In the long-term limit (not shown in Fig. 1, but see, e.g. [8]), the periodic pattern gradually decays. Adjacent domain borders form closed loops which shrink and finally disappear. In the Fourier spectrum, this process manifests itself in a broadening and a shift of the peaks towards longer wavelengths.

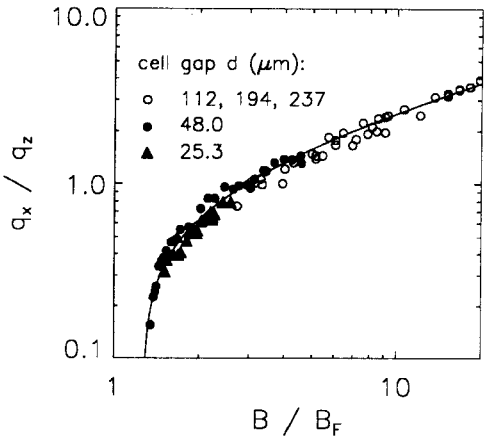

Figure 2: Wave numbers experimentally observed in Mi5 at 23.7°C for five different cell gaps d.
$B_F = \pi/d\ (\mu_0 K_2/\Delta\chi)^{1/2}$, $q_z = \pi/d$
The solid line gives a fit to Eq.(3) with $\alpha = 0.86$, $\eta = 0.23$, and $\kappa = 2.30$.

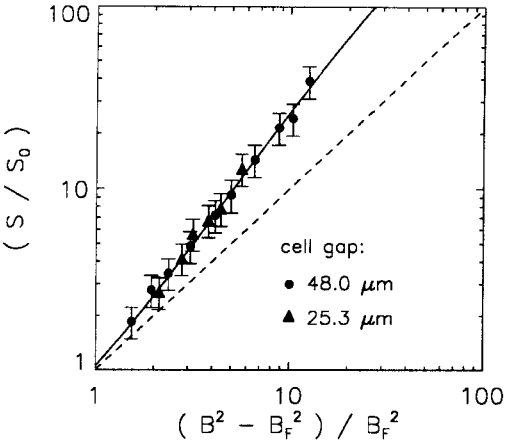

Figure 3: Exponential growth rates of the periodic patterns in Mi5 at 23.7°C for two different cell gaps. The solid line was calculated from Eq.(2) with the fit parameters of Fig. 2. The dashed line belongs to a homogeneous reorientation.

The wavelengths of the structures show a critical behaviour in dependence on magnetic field strength. They diverge in the vicinity of some threshold field for the pattern formation. Measured wave numbers vs. magnetic field are shown in Fig. 2. A universal relationship is found if the wavelengths are scaled with the cell thickness, and the external field strengths with the corresponding twist Fréedericksz field B_F.

In order to find a measure of the rise time of the structures, we have determined the contrast ratio of the images in dependence upon time. By calculation of the optical transmission, the contrast ratio is found to be proportional to the twist deformation amplitude in the small angle limit. The growth rates determined for the optical contrast are therefore assumed to be identical with those of the director structures. Details will be published elsewhere [11]. In Fig. 3, growth rates obtained from two

sample cells of different thicknesses are given as a function of the magnetic field. As already the wavelengths, the growth rates also obey a universal function for the cells investigated if they are scaled with the zero field relaxation rate $s_0 = K_2\pi^2/\gamma_1 d^2$. The observed periodic patterns increase considerably faster than a homogeneous twist reorientation. The homogeneous reorientation rate is given for comparison by a dashed line in Fig. 3. Only if the magnetic field approaches the critical field for pattern formation, the pattern growth rate approaches that of the homogeneous reorientation.

THEORY

DYNAMIC STRUCTURES

We consider a nematic LC contained in a planar cell with strong homogeneous anchoring at the surfaces. After the application of an external magnetic field perpendicular to $\vec{n}_0$, the director field is in an instable equilibrium and small thermal director fluctuations grow exponentially in the destabilizing field. Their growth rates s are inversely proportional to some effective viscosity of the particular distortion mode under consideration. Due to coupling between director and flow velocity gradients, a spatially inhomogeneous reorientation of the director ($q \neq 0$) may be connected with a considerably reduced effective viscosity as compared to the homogeneous director reorientation ($q = 0$). Elastic forces, however, damp the growth rates of modes with short wavelengths. Some optimum mode exists with maximum exponential director reorientation rate. This fastest growing mode that finally dominates all other modes can be calculated by means of a linear stability analysis (LSA) of the *Leslie-Ericksen* equations [1]. Its wavelength depends on the visco-elastic parameters of the LC, the magnetic field strength and boundary conditions. In bulk samples, the wave vector of this mode is along the initial director $\vec{n}_0$ determined by the magnetic field direction before the flip experiment. In thin cells, the wave vector has a second non-zero component q_z normal to the cell plane as a consequence of the boundary conditions. The equations can be generalized by proper scaling of q_x/q_z and B/B_F.

Figures 4a,b compare results of the linear stability analysis of the director reorientation in bulk samples ($- \cdot -$) and for the dynamic twist Fréedericksz transition (—). In bulk samples, long wavelengths of large amplitudes would be dominating if the velocity field were not damped by inertia. Inertia terms are negligible for Fréedericks cells at moderate magnetic fields where the boundary conditions (strong director

anchoring and no slip) strongly influence the mode evolution (dashed line in Fig. 4b). Periodic patterns form only at magnetic fields exceeding some threshold field $B_s > B_F$ in the latter systems.

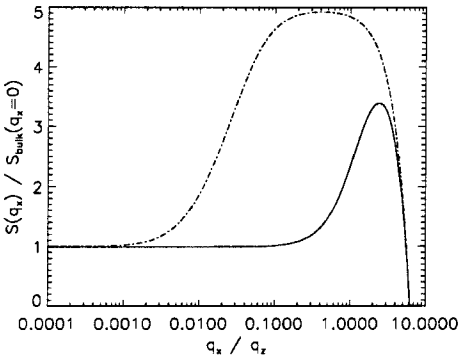

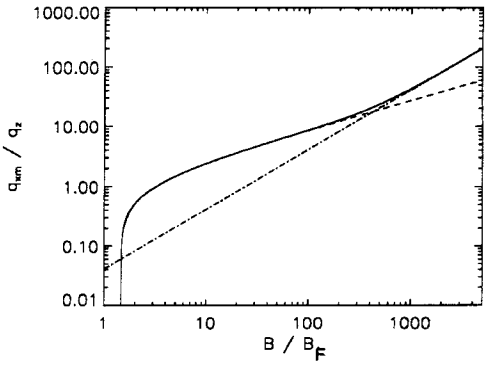

Figure 4a)
Growth rates of different modes at $B = 10B_F$ as calculated from LSA: twist Fréedericksz transition (—), reorientation in bulk samples (– · –). ($s_{bulk}(q_x = 0) = \Delta\chi B^2/(\mu_0\gamma_1)$).

b)
Wave vector of the fastest growing mode calculated from LSA as function of the magnetic field: exact solution (—), bulk approximation (– · –) and neglection of the inertia term (- - -).

Bulk functions have been formally scaled for comparison. Viscoelastic parameters of 5CB at 25°C have been assumed.

The linearized equations of motion are solved assuming decoupled director and mass flux modes and homogeneity in the direction of the magnetic field. The director inertia term is neglected. We arrive at Eq. (1) for the exponential growth rate of director modes in the dynamic twist Fréedericksz transition:

$$s(q_x, q_z, B) = \frac{1}{2\rho\gamma_1}\left\{\sqrt{F^2 + 4\rho\gamma_1\left(\frac{\Delta\chi}{\mu_0}B^2 - q_z^2K_2 - q_x^2K_3\right)(\eta_a q_z^2 + \eta_c q_x^2)} - F\right\} \quad (1)$$

$$\text{with} \quad F = A_1 q_x^2 + A_2 q_z^2 - \rho\tfrac{\Delta\chi}{\mu_0}B^2,$$
$$A_1 = \eta_c\gamma_1 - \alpha_2^2 + \rho K_3 \approx \eta_c\gamma_1 - \alpha_2^2 \quad \text{and} \quad A_2 = \gamma_1\eta_a + \rho K_2 \approx \gamma_1\eta_a,$$
$$\gamma_1 = \alpha_3 - \alpha_2,\ \eta_a = \alpha_4/2,\ \eta_c = 1/2(\alpha_4 + \alpha_5 - \alpha_2),\ .$$

ρ is the mass density, α_i are the Leslie viscosity coefficients and K_2, K_3 the elastic constants for twist and bend deformation, resp., of the nematic phase. In the limit $\frac{B}{B_F} \ll \sqrt{\frac{\gamma}{\rho K}}$ (γ beeing an averaged viscosity and K an averaged elastic constant)

inertia can be neglected. Eq. (1) simplifies to Eq. (2):

$$s(q_x, q_z, B) = \frac{\frac{\Delta\chi}{\mu_0} B^2 - K_2 q_z^2 - K_3 q_x^2}{\gamma_1 - \alpha_2^2 / \left(\eta_c + \eta_a \left(q_x/q_z\right)^{-2}\right)} \tag{2}$$

which was already derived by Lonberg and Fraden [5,6].

The fastest growing mode is found by maximizing s with respect to q_x and q_z. Its wave vector is given by Eq. (3) if inertia effects are negligible as in our experiments.

$$\left(\frac{B}{B_F}\right)^2 = \left(\frac{1-\alpha}{\eta\alpha}\kappa\right) Q^4 + \left(\frac{2\kappa}{\alpha}\right) Q^2 + \left(1 + \frac{\kappa\eta}{\alpha}\right) \quad \text{with} \quad Q = \frac{q_x}{\pi/d} = \frac{2d}{\lambda}. \tag{3}$$

$$\alpha = \frac{\alpha_2^2}{\gamma_1 \eta_c}, \; \eta = \frac{\eta_a}{\eta_c}, \quad \text{and} \quad \kappa = \frac{K_3}{K_2}.$$

This equation has real roots for $B > B_S$ with

$$B_S = \sqrt{\left(1 + \frac{\kappa\eta}{\alpha}\right)} B_F.$$

The periodicities of the patterns observed in our experiments are in excellent agreement with the predictions from LSA. The solid line in Fig. 2 gives the best fit to Eq. (3). The parameters $\alpha = 0.86$, $\eta = 0.23$ and $\kappa = 2.30$ have been obtained from the fit. κ was found to be 2.285 from previous independent measurements of the elastic constants [8]. Both values agree well within the experimental errors. We compared the experimentally determined growth rates of the structures with those predicted from the LSA using the parameters obtained from the wavelength fit. The agreement was excellent again, as the solid line in Fig. 3 indicates.

METASTABLE STRUCTURES

The linear analysis holds for the initial evolution of the director and flow fields. With increasing modulation amplitudes, non-linear terms enter the hydrodynamic equations. Finally, the dynamic pattern formation process results in a modulated metastable director field of domains separated by splay-bend inversion walls (Fig. 5a).

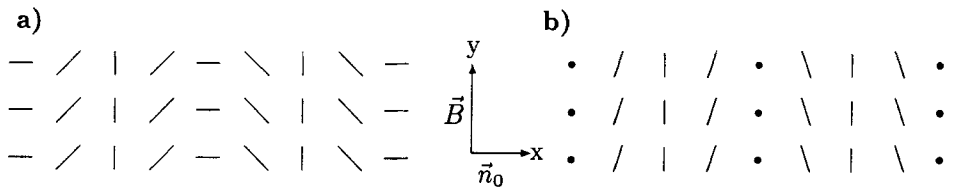

Figure 5:
Director field of the transient structures in the sample midplane as seen from above: domains of opposite director reorientation separated by planar splay-bend inversion walls **(a)** (cf. Fig. 1, top), and by out-of-plane twist inversion walls **(b)** (cf. Fig. 1, bottom).

Applying a minimization procedure for the free energy and using an appropriate model for the director field, numerical calculations have shown that the in-plane splay-bend inversion walls become instable with respect to an out-of-plane tilt of the director when the magnetic field exceeds some critical value B_T [8]. The splay-bend walls transform into energetically favoured twist walls where splay and bend deformations are partially replaced by lower energy twist ($K_2 < K_1 \approx K_3$). This is in excellent agreement with our experimental observations (see Fig. 1) and with investigations on lyotropic and polymer systems reported in the literature (see e.g. [12]). The periodically modulated non-planar director field leads to strong diffraction effects and light focussing as is known from Williams domains.

CONCLUSIONS

We have investigated the director field in transient textures during the twist reorientation of low molecular mass nematic LC. Wavelengths and wavevectors of the patterns have been analyzed by optical methods.

Two types of structures can be distinguished by their optical appearance. The planar deformation mode can be described by a linear stability analysis which predicts a critical field B_s and a characteristic field and cell thickness dependence of the wavelength. The planar structures can be observed optically in thin cells with crossed polarizers at 0° to $\vec{n}_0$ and a $\lambda/4$-plate in 45° orientation inserted. The optical contrast between domains of opposite twist is proportional to the twist angle in the midplane of the cell at small deformations. Therefore, we are able to determine the director reorientation rate from the evolution of the texture contrast in time.

The appearance of twist inversion walls in the long-term limit can be described well by

means of a free energy analysis [8] where another threshold field $B_T > B_s$ is predicted that is confirmed experimentally. These structures have been observed in all cells at sufficiently high magnetic fields. Their optical diffraction patterns are visible without polarizers. Splay-bend walls at low fields can be converted to twist-bend walls of the same spacing by increasing the field after the formation of the planar patterns.

The wave vectors of the patterns have been determined by means of a two-dimensional Fourier transform of the transmission images. We expect the wavelength of the selected modes to be constant in time as long as the linear theory holds. Our experiments show that the wavelengths of the observed transient patterns are almost constant during their evolution. In particular at fields well above B_F, a small increase of the wavelengths of about 10..20% (which is only slightly above experimental error) is observed in the course of the experiment. In the fit, we have used the initial q_x values.

The evolution of the periodic planar splay-bend deformations can be observed optically when the the twist deformation amplitudes are of the order of 10°. In this early stage, the application of LSA should be justified. Hence we are confident that the wavelengths found in our experiments can be used to calculate viscoelastic coefficients of the nematic. For the investigated mixture Mi5, we found $\alpha = 0.86$, $\eta = 0.23$, and $\kappa = 2.30$ The good agreement of the experimental data of growth rates with those calculated using the parameters of the wavelength fit strongly supports this result.

This work was supported by DFG grant No. *Sta 425/1-1*. The authors are indebted to Dr. W. Weissflog for the supply of LC material.

REFERENCES

1. P. de Gennes; *The Physics of Liquid Crystals.* Clarendon Press Oxford (1974).
2. G. Srajer, S. Fraden, and R. B. Meyer; Phys. Rev. **A 39**, 4828 (1989).
3. E. Guyon, R.Meyer, and J. Salan; Mol. Cryst. Liq. Cryst. **54**, 261 (1979).
4. A.J. Hurd, S. Fraden, F. Lonberg, and R. B. Meyer; J. de Physique",**46**, 905 (1985).
5. F. Lonberg, S. Fraden, A.J. Hurd, and R.B. Meyer; Phys. Rev. Lett. **52**, 1903 (1984).
6. S. Fraden, A.J. Hurd, R.B. Meyer, M. Cahoon, and D.L.D. Caspar; J. de Physique **46**, C3–85 (1985).

7. F. Sagues and F. Arias and M. San Miguel; Phys. Rev. A **37**, 3601 (1988).
8. M. Grigutsch, N. Klöpper, H. Schmiedel, R. Stannarius; Phys. Rev. E (1994) (*in press*)
9. M. Grigutsch, N. Klöpper, H. Schmiedel, R. Stannarius, H. Gotzig, F. Noack; Proc. 23. Freiburger Arbeitstagung Flüssige Kristalle (1994).
10. R. Stannarius, W. Günther, M. Grigutsch, A. Scharkowski, W. Wedler, and D. Demus; Liq. Cryst., **9**, 285 (1991).
11. M. Grigutsch, and R. Stannarius *in preparation.*
12. N. Schwenk, and H. W. Spiess. J. de Physique II, **3**, 867 (1993).